

Computational Analysis of Optimal Sensor Position in Indoor Environment

M. V. Shyla*

Department of Mathematics, Sathyabama University, Chennai-600119, India;
shylamv@yahoo.com

Abstract

Background/Objectives: Placement of sensors plays an important role in getting an early warning about the contaminant. In reality, unsteady flow conditions are dominant. Hence this paper focuses on optimal sensor position under unsteady flow conditions. **Method:** Computation analysis of airflow around circular sensors fixed at different positions under unsteady state condition with laminar flow is performed in indoor environment using Finite volume method. **Results:** This CFD analysis helps to calculate and visualize the unknown parameters namely velocity and pressure at every point around the sensors. **Conclusion:** The results obtained in this study can be applied in locating the optimal sensor position in indoor environment.

Keywords: CFD Analysis, Finite Volume Method, Laminar, Optimal Sensor Position, Unsteady Flow

1. Introduction

Today there are lots of sensors available in the market. On the other hand accidents are still going on. Early warning can prevent such dangerous situations. Efficiency of sensors can be increased by optimal sensor position. Researchers prefer CFD to obtain more accurate results¹⁻⁶. CFD analysis is performed to identify and fix optimal sensor position under steady state conditions^{7,8}. In reality, unsteady flow conditions prevail. Hence it is required to analyze flow patterns in unsteady state.

In this paper, we extend our study of airflow patterns around circular sensors in 3 models with laminar flow by considering unsteady state conditions. CFD models are developed by fixing sensors at different locations in an indoor set up and finally 3 unique models are derived and compared to obtain the optimal sensor position.

The paper is organized as follows. The mathematical formulation is presented in the first part. The methodology is given in the second part. The results are discussed in the

third part. The conclusions of this study are presented in the last part.

2. Mathematical Formulation

2.1 Governing Differential Equation

The governing differential equations for an unsteady, incompressible flow are given by Navier-Stokes system of equations.

Equation of continuity:

$$\frac{\partial u}{\partial x} + \frac{\partial v}{\partial y} = 0 \quad (2.1)$$

x-momentum equation:

$$\rho \left(\frac{\partial u}{\partial t} + u \frac{\partial u}{\partial x} + v \frac{\partial u}{\partial y} \right) = -\frac{\partial p}{\partial x} + \mu \left(\frac{\partial^2 u}{\partial x^2} + \frac{\partial^2 u}{\partial y^2} \right) \quad (2.2)$$

* Author for correspondence

$$\rho \left(u \frac{\partial v}{\partial x} + v \frac{\partial v}{\partial y} \right) = - \frac{\partial p}{\partial y} + \mu \left(\frac{\partial^2 v}{\partial x^2} + \frac{\partial^2 v}{\partial y^2} \right) \quad (2.3)$$

$\vec{q} = u\vec{i} + v\vec{j}$ is the velocity vector. u and v denotes the velocity components in the x & y directions respectively, p denotes pressure, ρ denotes density, and μ denotes coefficient of viscosity.

The cartesian coordinates (x, y) is transformed to curvilinear coordinates (ξ, η) and the problem is solved. The solution is converted back and expressed in terms of cartesian coordinates (x, y) .

2.2 Boundary Conditions

A two dimensional, viscous, incompressible, laminar flow of air is simulated around circular sensors under unsteady state conditions. The operating pressure is taken as 101325 Pascals. All body forces are ignored. The inlet velocity of 0.02m/s is applied. The walls are considered to be rigid. The physical properties of air namely density $\rho=1.225\text{kg/m}^3$ and coefficient of viscosity $\mu=1.7894\text{e-}05\text{ kg/m-s}$ are taken for analysis.

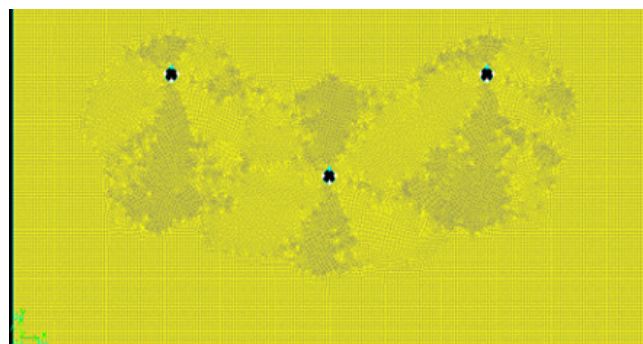


Figure 1a. Grid of Model 1

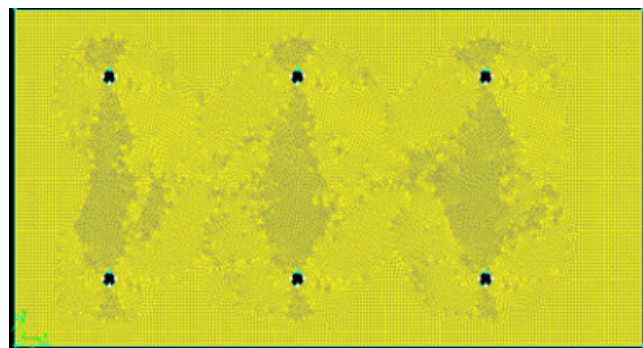


Figure 1b. Grid of Model 2



Figure 1c. Grid of Model 3

3. Methodology

The CFD model is generated using the CFD software, Gambit (Figure1a, Figure1b, Figure1c). The dimensions of the indoor building are considered as 100m and 50m in the x and y directions respectively with circular sensor radius 1 m. The sensors in 3 models are located as follows. Model 1 has 3 sensors centered at $(25, 40)$, $(50, 25)$, and $(75, 40)$. Model 2 has 6 sensors with centre at $(15, 10)$, $(45, 10)$, $(75, 10)$, $(15, 40)$, $(45, 40)$, and $(75, 40)$. Model 3 has 3 sensors positioned with centre at $(25, 25)$, $(75, 10)$, and $(75, 40)$. Finite volume method is applied to obtain the velocity profile, pressure distribution and streamline pattern.

3.1 Discretization

The quadrilateral pave mesh is generated with interval size 0.25 for all the models. The number of mesh faces and nodes for each model are presented (Table 1). The two dimensional mesh generated using Gambit software is exported to fluent software for analysis.

Table 1. Discretization

Model	No. of Nodes	No. of mesh faces
1	82703	82066
2	83602	82929
3	82814	82177

The integral form of partial differential system of equations given in equations 2.1, 2.2 and 2.3 is discretized by upwind differencing scheme over each control volume and they are transformed to algebraic system of equations as follows:

$$\frac{(\rho u A)_e - (\rho u A)_w}{\Delta x} + \frac{(\rho v A)_n - (\rho v A)_s}{\Delta y} = 0 \quad (3.1)$$

$$\begin{aligned}
 \frac{(\rho u^{n+1} A)_e - (\rho u^{n+1} A)_w}{\Delta t} + \frac{(\rho \mu)_e u_e - (\rho \mu)_w u_w}{\Delta x} + \frac{(\rho \mu)_n v_n - (\rho \mu)_s v_s}{\Delta y} &= \frac{(p_w - p_e)}{\Delta x} \Delta V_u + \\
 &\left\{ \left[\frac{\left(\mu \frac{\partial u}{\partial x} \right)_e - \left(\mu \frac{\partial u}{\partial x} \right)_w}{\Delta x} \right] + \left[\frac{\left(\mu \frac{\partial u}{\partial y} \right)_n - \left(\mu \frac{\partial u}{\partial y} \right)_s}{\Delta y} \right] \right\} \Delta V_u \\
 \frac{(\rho v^{n+1} A)_n - (\rho v^{n+1} A)_s}{\Delta t} + \frac{(\rho \mu)_e u_e - (\rho \mu)_w u_w}{\Delta x} + \frac{(\rho \mu)_n v_n - (\rho \mu)_s v_s}{\Delta y} &= \frac{(p_s - p_n)}{\Delta y} \Delta V_v + \\
 &\left\{ \left[\frac{\left(\mu \frac{\partial v}{\partial x} \right)_e - \left(\mu \frac{\partial v}{\partial x} \right)_w}{\Delta x} \right] + \left[\frac{\left(\mu \frac{\partial v}{\partial y} \right)_n - \left(\mu \frac{\partial v}{\partial y} \right)_s}{\Delta y} \right] \right\} \Delta V_v
 \end{aligned}
 \tag{3.2}$$

The equations 3.1 and 3.2 represent discretized Navier Stokes equation along the x direction and y directions respectively where ΔV_u and ΔV_v are the u-control volume and v-control volume respectively, A is the area, e is the node to the east of u-cell, w is the node to the west of u-cell, n is the node to the north of v-cell and s is the node to the south of v-cell.

Semi-Implicit Method for Pressure Linked Equations known as SIMPLE algorithm is used to solve the discretized equations. 500 iterations were performed by taking time step as 10 seconds.

The unknown pressure values p and the velocity magnitudes are computed.

3.2 Error Analysis and Validation

Grid validation is done for different models. The mass flow rate at the inlet and outlet is 1.225 kg/s. Conservation of mass and the convergence of the solution correct to three decimal places are monitored.

3.3 Future Scope

This study can be extended to unsteady state with different toxic chemicals.

4. Analysis of Results

Viscous flow of air around the circular sensors has been considered. The flow pattern around the circular sensors

placed at different positions is seen from the figures presented in this study.

4.1 Velocity Profile

The velocity magnitude at every point around the circular sensors is displayed corresponding to different colors starting from blue to red. Blue color is an indication of very low velocity region. Red color refers to very high velocity region. Low velocity region is observed along the downstream and upstream sides (Figure 2a, Figure 2b, Figure 2c) and high velocity region is observed in the region perpendicular to the circular sensors^{7,8}. Low velocity indicates the stagnation of fluid particles which signifies sensing.

In Model 1, the velocity magnitude corresponding to the green colour is 1.22e-02m/s only for two sensors but different for the last sensor (Figure 2a). For Model 2, (Figure 2b) with respect to the blue colour, it is 1.37e-03 m/s in the right side of the first 2 sensors arranged vertically. Considering the case of Model 3, regarding the red colour which is 2.73e-02 m/s (Figure 2c) on the top of every sensor.

4.2 Pressure Distribution

The pressure distribution at every point around the circular sensors is given corresponding to different colours starting from blue to red. Blue is used to represent very low pressure region. Red is used to indicate very

high pressure region. High pressure region is observed (Figure 3a, Figure 3b, Figure 3c, Figure 3d, Figure 3e) on the left side of the sensors^{7,8}. The pressure distribution in 3 models is compared.

In Model 1, the velocity magnitude corresponding to the red colour is 2.27×10^{-4} pascal in the left side of the first sensor and middle sensor and 1.96×10^{-4} pascal for the last sensor. There is a deviation of pressure values in the case of Model 1 (Figure 3a).

In Model 2, the pressure corresponding to the red colour is 2.18×10^{-4} pascal in the left side of the first 2 sensors arranged vertically and $1.19 \times 10^{-4} \text{m/s}$ for the remaining 4 sensors. There is a slight variation of pressure in the case of Model 2 (Figure 3b).

In Model 3, the pressure corresponding to the red colour is 2.22×10^{-4} pascal in the left side of all three sensors. There is no change in the pressure value in the case of Model 3 (Figure 3c).

4.3 Streamline Pattern

Streamline pattern presented in (Figure 4) indicates the direction of flow of fluid particles. Length of the vector determines the velocity at that point. It is observed that high velocity region is represented by bigger arrows and low velocity region by smaller arrows. Iteration plots are given (Figure 5a, Figure 5b, and Figure 5c). The solution converges at 53rd iteration for Model 1 and Model 2, 54th iteration for Model 3.

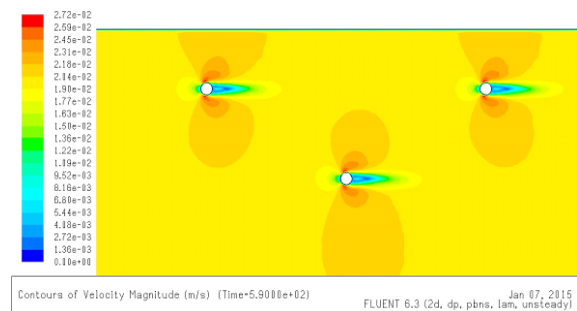


Figure 2a. Velocity Profile around circular sensors in Model 1.

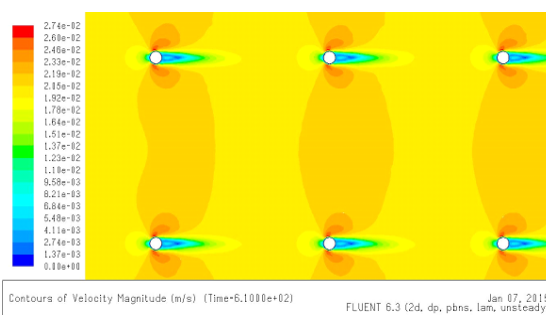


Figure 2b. Velocity Profile around circular sensors in Model 2.

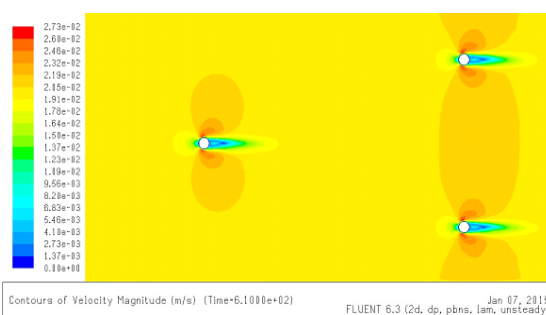


Figure 2c. Velocity Profile around circular sensors in Model 3.

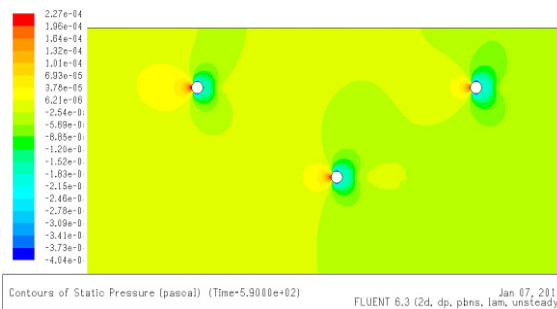


Figure 3a. Pressure Distribution around circular sensors in Model 1.

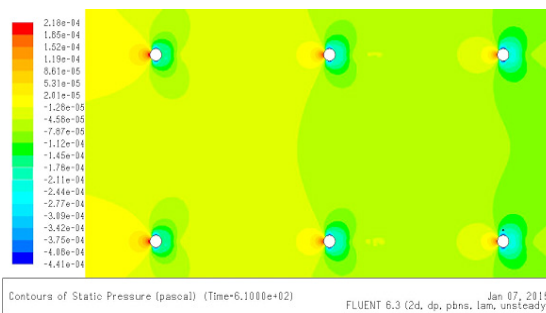


Figure 3b. Pressure Distribution around circular sensors in Model 1.

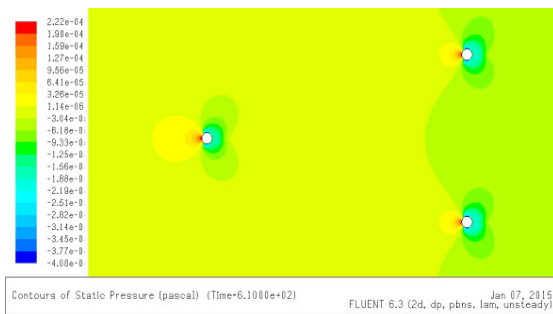


Figure 3c. Pressure Distribution around circular sensors in Model 3.

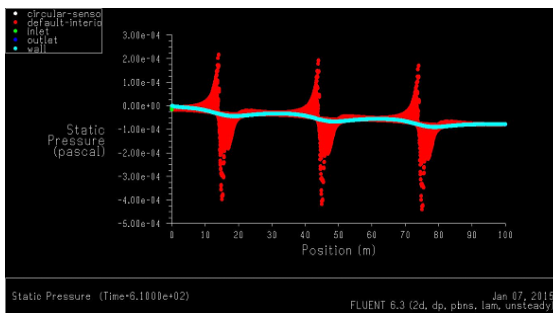


Figure 3d. Pressure plot in Model 2.

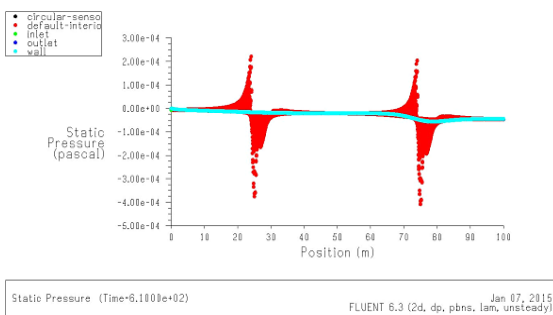


Figure 3e. Pressure plot in Model 3.

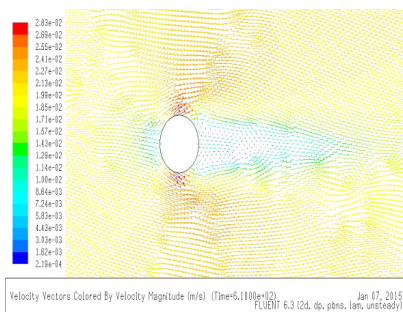


Figure 4. Streamline Pattern.

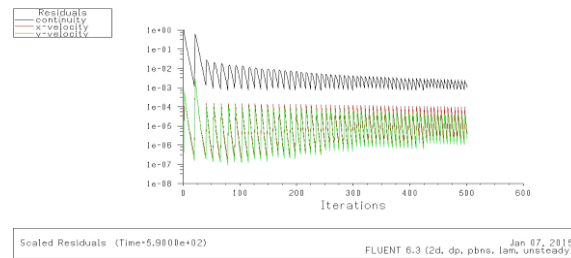


Figure 5a. Velocity iteration plot for laminar flow around circular sensors in Model 1.

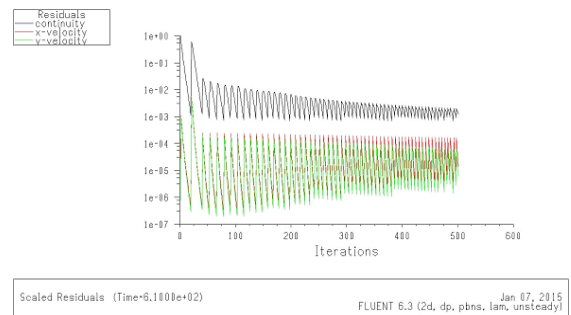


Figure 5b. Velocity iteration plot for laminar flow around circular sensors in Model 2.

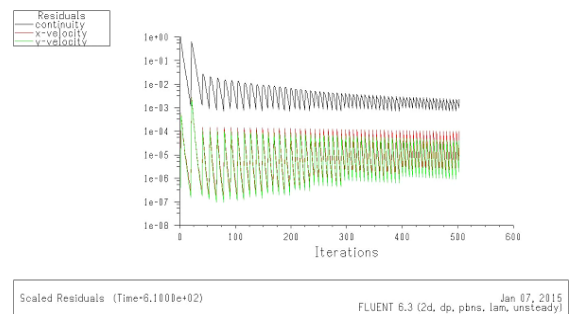


Figure 5c. Velocity iteration plot for laminar flow around circular sensors in Model 3.

5. Conclusion

A two dimensional, laminar, viscous, incompressible flow field around circular sensors in 3 unique models has been analyzed under unsteady state conditions. Low velocity region and high pressure region is an implication of sensing. Since there is no deviation in the velocity magnitude and pressure values around the circular sensors used in Model 3, the efficiency of sensing is more in the case of Model 3 arrangement. Hence this information derived from this study can be applied for understanding optimal sensor position in any real life scenario.

6. References

1. liu Z. Odour source Localization using multiple plume tracing mobile robots. [Ph.D. Thesis]. Australia: University of Adelaide; 2000. p. 1–33.
2. Ishida H, Tsuruno M, Yoshikawa K, Moriizumi T. Spherical gas sensor array for three dimensional plume tracking. 11th International Conference on Advanced Robotics; Coimbra, Portugal: 2003. p. 369–74.
3. Obenschain K, Boris J, Patnaik G. Using CT-ANALYSTTM to optimize sensor placement. Proceedings of SPIE 2004. 2004; 5416:14–20.
4. Zhang T, Chen Q. Novel air distribution systems for commercial aircraft cabins. Build Environ. 2007; 42(4):1675–84.
5. Liu Z, Lu. Odor source localization in complicated indoor environments. 10th International Conference on Control, Automation, Robotics and Vision; Adelaide, South Australia: University of Adelaide; 2008:371–7.
6. Shyla MV, Naidu KB, Vasanth Kumar G. Optimization of sensor position on Different surfaces using CFD Analysis for reducing accidents caused by emission of toxic gas in Industries. IEEE conference “International conference on Advance Computing-2013” ICOAC-13; Chennai, India: Anna University; p. 1–8.
7. Shyla MV, Naidu KB, Kumar GV. Identification of sensor position using CFD Simulation. Elsevier conference “International conference on Mathematical Sciences ICMS-2014; Sathyabama University: 2014 July 19. p. 302–7. ISBN 978-93-5107-261-4.
8. Shyla MV, Naidu KB, Kumar GV. Fixing sensor position using CFD analysis for trace detection of toxic gases. Indian journal of science and technology. 2014; 7(12):1987–98.